The Astrophysical Journal, 889:133 (10pp), 2020 February 1 https://doi.org/10.3847/1538-4357/ab63c9

Periodic Modulation: Newly Emergent Emission Behavior in Pulsars

Rahul Basu[1,2], Dipanjan Mitra[2,3], and Giorgi I. Melikidze[2,4]
[1] Inter-University Centre for Astronomy and Astrophysics, Pune, 411007, India; rahulbasu.astro@gmail.com
[2] Janusz Gil Institute of Astronomy, University of Zielona Góra, ul. Szafrana 2, 65–516 Zielona Góra, Poland
[3] National Centre for Radio Astrophysics, Tata Institute of Fundamental Research, Pune 411007, India
[4] Evgeni Kharadze Georgian National Astrophysical Observatory, 2a, Al. Kazbegi Ave., Tbilisi 0160, Georgia
Received 2019 July 21; revised 2019 November 27; accepted 2019 December 13; published 2020 January 31

Abstract

Periodic modulations are seen in normal pulsars ($P > 0.1$ s) over timescales ranging from a few seconds to several minutes. Such modulations have usually been associated with the phenomenon of subpulse drifting. A number of recent studies have shown subpulse drifting to exhibit very specific physical characteristics: (i) drifting is seen only in conal components of the pulse profile and is absent in central core emission; (ii) drifting pulsars are distributed over a narrow range of spin-down energy loss ($\dot{E}$), where pulsars with $\dot{E} < 2 \times 10^{32}$ erg s^{-1} show this behavior; and (iii) drifting periodicity (P_3) is anti-correlated with $\dot{E}$, such that pulsars with lower values of $\dot{E}$ tend to have longer P_3. These detailed characterizations of drifting behavior, on the other hand, also revealed the presence of other distinct periodic modulations, which can be broadly categorized into two types, periodic nulling, and periodic amplitude modulation. In contrast to drifting, these periodic phenomena are seen across the entire profile in both the core and conal components simultaneously and are not restricted to any specific $\dot{E}$ range. In this work we have assembled an exhaustive list of around 70 pulsars that show such periodic modulations, 22 of which were newly detected using observations from the Giant Meterwave Radio Telescope and the remaining compiled from past publications. The presence of such a significant group in the pulsar population suggests periodic modulations to be newly emergent phenomena in pulsars, with a physical origin that is distinct from that of subpulse drifting.

Unified Astronomy Thesaurus concepts: Radio pulsars (1353); Pulsars (1306)

Supporting material: figure sets

1. Introduction

Radio emission from normal period pulsars ($P > 0.1$ s) shows variations in their single pulses that exhibit different periodicities. Periodic behavior over timescales of several hundred pulses is studied using longitude-resolved fluctuation spectra (LRFS, Backer 1970a, 1973). LRFS requires single pulse sequences to be arranged in the form of a pulse stack, which is a two-dimensional representation with pulse longitude along the abscissa and every subsequent period placed along the ordinate. Fourier transforms are carried out along each longitude range of the pulse stack to form LRFS. Single pulses are composed of one or more components known as subpulses. Peak frequency in the fluctuation spectra represents periodicity of subpulse repetition at any given pulse longitude. Phase variations corresponding to the peak amplitude indicate the time delay with which a subpulse appears with respect to a specific reference longitude.

Periodic modulations have been studied in great detail in the literature, with Ruderman & Sutherland (1975) suggesting subpulse drifting as the primary mechanism for such variations. However, detailed phenomenological studies in the recent past have revealed other likely sources for periodic behavior in single pulses. We present a careful distinction between these possibilities in the discussion below.

1.1. Subpulse Drifting

The phenomenon of subpulse drifting is associated with systematic variations of subpulses within a pulse window (Drake & Craft 1968). Detailed studies of subpulse drifting in a large number of pulsars (Rankin 1986; Gil & Sendyk 2000; Deshpande & Rankin 2001; Weltevrede et al. 2006, 2007; Basu et al. 2016, 2019a; Basu & Mitra 2018a) reveal two important characteristics: evolution of drift pattern with line-of-sight (LOS) geometry, where the drifting is different for each component in profile, and dependence of drifting periodicity (P_3) on spin-down energy loss ($\dot{E}$).

Classification of profile types can be used to understand the evolution of drifting with LOS geometry. The average radio emission beam is expected to consist of a central core component, surrounded by two concentric conal rings (Rankin 1990, 1993). The observed profile diversity is believed to be related to a different LOS traversing the emission beam. When the LOS cuts across the edge of the beam, conal single (S_d) profiles are seen. As the LOS traverses progressively more interior regions of beam, conal double (D), conal triple ($_c$T), and conal quadruple ($_c$Q) profile classes are observed. Core-dominated profiles, viz., core single (S_t), core-cone triple (T), and core-double cone multiple (M) classes are expected to arise due to the central LOS traversing the emission beam. In some pulsars with core emission, one of the conal pairs is too weak to be detected and they are classified as $T_{1/2}$.

Subpulse drifting is a strictly conal phenomenon, with no drifting seen in the core component (Rankin 1986). In addition, drifting behavior also evolves from the outer edge to the central regions of the emission beam. Systematic large-scale phase variations are seen across the entire profile in the S_d and D profile classes. On the other hand. phase variations for each conal component in the $_c$T and $_c$Q profiles are usually different and show jumps and reversals from one component to another. In most M profiles drifting is largely phase-stationary in the outer conal components, but shows significant phase changes in the inner cones (Basu et al. 2019a, 2019b).

Subpulse drifting shows a clear dependence on $\dot{E}$, which is different from other periodic behavior. Drifting is seen in

pulsars with $\dot{E} < 5 \times 10^{32}$ erg s^{-1}. In addition, a correlation can also be inferred between drifting periodicity (P_3) and $\dot{E}$. If the periodicity measured in LRFS is not considered to be aliased, pulsars with low $\dot{E}$ generally have longer P_3 than pulsars with higher $\dot{E}$. This anti-correlation becomes stronger under the assumption that subpulse motion is lagging behind corotation speed. In this scenario negative drifting with subpulse motion from the trailing to the leading edge of the profile has $P_3 > 2P$, and positive drifting with subpulse motion toward the trailing edge has $P < P_3 < 2P$. The estimated dependence is given as $P_3 \propto \dot{E}^{-0.6\pm0.1}$ (Basu et al. 2016; Ritchings & Lyne 1975).

Subpulse drifting is associated with non-stationary plasma flow in the inner acceleration region (IAR) of pulsars, which is best explained using a partially screened gap model (PSG; Gil et al. 2003; Szary et al. 2015). The PSG model considers a steady flow of ions from the stellar surface, which screens the electric field in the IAR by a screening factor (η):

$$\eta = 1 - \rho_i/\rho_{\rm GJ}; \quad \rho_{\rm GJ} = \boldsymbol{\Omega} \cdot \boldsymbol{B}/2\,c. \tag{1}$$

Here, ρ_i is density of ions and $\rho_{\rm GJ}$ is the Goldreich–Julien density (Goldreich & Julian 1969). The plasma responsible for radio emission is generated in IAR in the form of sparking discharges (Ruderman & Sutherland 1975). Sparks do not corotate with the star, but lag behind corotation speed, which results in subpulse drifting.

In the presence of PSG the drift speed of sparks ($v_{\rm sp}$) can be expressed as (Basu et al. 2016)

$$v_{\rm sp} = \eta(E/B)c, \tag{2}$$

where B is the magnetic field and E is the corotation electric field. The subpulses can be associated with spark motion in IAR. It is speculated that IAR is packed with circular sparks, which are also equidistant, represented by size h (Gil & Sendyk 2000). The time of the repetition of sparks at any longitude, which is also drifting periodicity (P_3), is estimated as

$$P_3 = 2h/v_{\rm sp}. \tag{3}$$

When η is small ($\eta \sim 0.1$) it can be shown that P_3 in PSG is estimated as (Szary 2013)

$$P_3 = \frac{1}{2\pi\eta\cos\alpha}, \tag{4}$$

where α is the inclination angle between rotation and magnetic axes. The anti-correlation between P_3 and $\dot{E}$ can be derived from Equations (3) and (4) using basic physical approximations. When the full energy outflow from the polar cap is associated with $\dot{E}$ using factor ξ we obtain (Basu et al. 2016)

$$P_3 = 2 \times 10^{-9}\left(\frac{\gamma_0}{\xi}\right)\left(\frac{\dot{E}}{\dot{E}_1}\right)^{-0.5}, \tag{5}$$

where $\gamma_0 \sim 10^6$ is the Lorentz factor of primary particles in IAR, $\xi \sim 10^{-3}$–10^{-4} is the scaling factor obtained from the fraction of non-thermal X-ray emission (Becker 2009), and $\dot{E}_1 = 4 \times 10^{31}$ erg s^{-1}.

1.2. Other Periodic Modulations

Recent studies have revealed the presence of additional periodic behaviors seen in fluctuation spectra, which include periodic nulling (Herfindal & Rankin 2007) and periodic amplitude modulation. Periodic nulling is seen in conal as well as core-cone profiles, where the core components vanish along with cones in a periodic manner. This prompted Basu et al. (2017) to identify periodic nulling as a different phenomenon. In addition, certain pulsars with core emission show low-frequency modulation in intensity, where the core component also participates (Basu et al. 2016; Mitra & Rankin 2017). This behavior is known as periodic amplitude modulation.

There are clear differences between physical parameters of subpulse drifting and other periodic modulations. A significant number of pulsars showing this behavior have high $\dot{E}$ in excess of 5×10^{32} erg s^{-1}. Periodic nulling and periodic amplitude modulation are usually seen as low-frequency features in fluctuation spectra. The corresponding longer periodicities are not correlated with $\dot{E}$, unlike subpulse drifting.

The contrasting behavior of drifting and other periodic modulations is clearly illustrated in pulsars where both effects are seen in the pulse sequence (Basu et al. 2017, 2019a). In all such cases the low-frequency feature in fluctuation spectra can be identified as periodic modulation. One example is the pulsar B2003−08, with an M type profile, which has subpulse drifting and periodic nulling. Subpulse drifting is seen only in conal pairs, where the outer pairs have phase-stationary behavior and the inner pairs exhibit large-scale bi-drifting behavior. Periodic nulling is seen across entire profile as a phase-stationary behavior (Basu et al. 2019b). Another pulsar B1737+13, with an M type profile, exhibits both subpulse drifting and periodic amplitude modulation. Drifting only affects the conal components, but amplitude modulation is seen across all components (Force & Rankin 2010).

The physical mechanism of periodic modulations is still unknown, but is expected to be different from subpulse drifting. Subpulse drifting can be explained using standard physics of non-stationary flow in the PSG, as explained above. On the other hand, the origin of a number of other physical phenomena in pulsar radio emission cannot be explained using this standard model. In certain pulsars subpulses exhibit quasi-periodic structures that are also called microstructures. They likely originate due to temporal modulations of non-stationary plasma flow resulting in alternating radial emitting regions interspersed with relatively less bright parts (Mitra et al. 2015). However, the presence of such modulations requires variations in the plasma generation process in PSG, which are currently unknown.

Pulsar radio emission also shows the presence of nulling (Backer 1970b), and mode changing (Backer 1970c), where emission switches from one steady state to another. These phenomena are not periodic, with rapid transitions between different states (usually within a period), which switch back to the initial state after irregular intervals. A notable exception is the periodic swooshing events in pulsars B0919+06 and B1859+07 (Rankin et al. 2006; Wahl et al. 2016). Their physical origin, unlike drifting, also cannot be explained using the steady-state conditions in IAR, and requires changes in the plasma generation process that are still unexplored.

A detailed classification of subpulse drifting from a complete list of pulsars has been reported in Basu et al. (2019a). However, no equivalent study exists for periodic nulling and periodic amplitude modulation, which we plan to address in this work. We have carried out measurements of nulling and periodicities in a large number of pulsars, observed using the Giant Meterwave Radio Telescope (GMRT), as well as

Table 1
Estimations of Nulling and Modulation Periodicity

PSR	P (s)	N_p	NF (%)	N_T	$\langle$BL$\rangle$ (P)	$\langle$NL$\rangle$ (P)	f_p (cy/P)	FWHM (cy/P)	S_M (P/cy)	P_M (P)	Remarks
B0105+65	1.284	3020	...	...	...	...	...	...	...	...	No Nulls
B0138+59	1.223	1960	7.6 ± 1.0	89	19.0	2.8	0.023 ± 0.017	0.040	21.2	44 ± 30	Periodic Nulls
B0320+39	3.032	2073	0.7 ± 0.2	14	140.4	1.0	...	...	...	...	Short Nulls
B0355+54	0.156	13113	...	...	...	...	...	...	...	...	Low emission
B0402+61	0.595	3041	...	...	...	...	...	...	...	...	No Nulls
J0421−0345	2.161	1226	...	...	...	...	...	...	...	...	Low emission
B0447−12	0.438	2742	...	...	...	...	...	...	...	...	No Nulls
B0450−18	0.549	2738	...	...	...	...	0.064 ± 0.023	0.055	18.1	15.6 ± 5.7	Amp. Mod.
B0450+55	0.341	2658	...	...	...	...	0.111 ± 0.016	0.037	27.4	9.0 ± 1.3	Amp. Mod.
B0523+11	0.354	3436	...	...	...	...	...	...	...	...	No Nulls
B0559−05	0.396	3900	...	...	...	...	...	...	...	...	No Nulls
B0609+37	0.444	2049	...	...	...	...	...	...	...	...	Low emission
B0621−04	1.039	1357	...	...	...	...	0.0137 ± 0.0003	0.0007	313.5	73.1 ± 1.6	Low emission
B0727−18	0.510	3537	...	...	...	...	...	...	...	...	Low emission
B0740−28	0.167	3629	...	...	...	...	...	...	...	...	No Nulls
B0809+74	1.292	890	1.2 ± 0.4	6	145.2	2.0	...	...	...	...	Short Nulls
B0818−13	1.238	2425	0.9 ± 0.1	16	130.6	1.3	...	...	...	...	Short Nulls
B0820+02	0.865	1376	0.5 ± 0.2	7	181.1	1.0	...	...	...	...	Short Nulls
B0905−51	0.254	2358	...	...	...	...	...	...	...	...	No Nulls
B0906−17	0.402	2244	12.4 ± 1.1	...	...	...	...	...	...	...	Low emission
B0919+06	0.431	4100	...	...	...	...	...	...	...	...	No Nulls
B0932−52	1.445	1614	1.9 ± 0.1	30	48.7	1.5	0.029 ± 0.016	0.038	7.6	35 ± 19	Periodic Nulls
B1112+50	1.656	1977	34.8 ± 1.4	215	3.4	5.8	...	...	...	...	Med. Nulls
B1237+25	1.382	946	8.9 ± 1.0	40	21.2	2.1	0.039 ± 0.007	0.018	39.4	25.7 ± 4.9	Periodic Nulls
B1322+83	0.670	2672	...	...	...	...	...	...	...	...	Low emission
B1508+55	0.740	1784	5.2 ± 0.4	95	16.7	2.0	0.066 ± 0.032	0.076	2.6	15.1 ± 7.3	Periodic Nulls
B1510−48	0.455	2104	...	...	...	...	0.027 ± 0.003	0.007	57.9	36.6 ± 4.1	Low emission
B1540−06	0.709	5660	...	...	...	...	...	...	...	...	No Nulls
B1541+09	0.748	3035	...	...	...	...	0.066 ± 0.021	0.050	6.2	15.1 ± 4.8	Amp. Mod.
B1556−44	0.257	3550	...	...	...	...	...	...	...	...	No Nulls
B1601−52	0.658	4551	...	...	...	...	0.047 ± 0.015	0.036	1.7	21.4 ± 7.0	Low emission
B1604−00	0.422	3248	0.15 ± 0.07	...	...	...	0.029 ± 0.011	0.026	11.9	34 ± 13	Amp. Mod.
B1612+07	1.207	914	...	...	...	...	...	...	...	...	Low emission
B1642−03	0.388	1502	...	...	...	...	0.078 ± 0.032	0.075	5.9	12.8 ± 5.2	Amp. Mod.
J1650−1654	1.750	2162	...	...	...	...	0.016 ± 0.011	0.026	5.1	64 ± 45	Low emission
B1700−18	0.804	1849	...	...	...	...	0.023 ± 0.009	0.021	8.9	43 ± 15	Low emission
B1717−29	0.620	1850	...	...	...	...	...	...	...	...	No Nulls
B1718−02	0.478	3075	...	...	...	...	...	...	...	...	Low emission
B1742−30	0.367	1900	...	...	...	...	...	...	...	...	Low emission
B1804−08	0.164	1700	...	...	...	...	...	...	...	...	Low emission
B1822−09	0.769	2328	...	...	...	...	...	...	...	...	No Nulls
B1831−04	0.290	2000	...	...	...	...	...	...	...	...	Low emission
B1845−19	4.308	2223	27.2 ± 1.7	410	3.4	2.0	...	...	...	...	Short Nulls
B1851−14	1.147	1024	...	...	...	...	...	...	...	...	Low emission
J1857−1027	3.687	1000	>30	...	...	...	0.056 ± 0.033	0.077	11.2	18 ± 10	Periodic Nulls
B1857−26	0.612	1955	4.3 ± 0.5	198	8.6	1.2	...	...	...	...	Short Nulls
B1905+39	1.236	1124	10.0 ± 0.5	80	11.5	2.3	0.021 ± 0.011	0.026	26.9	47 ± 24	Periodic Nulls
B1907−03	0.505	1279	...	...	...	...	...	...	...	...	No Nulls
B1929+10	0.227	1824	...	...	...	...	0.088 ± 0.006	0.014	33.0	11.4 ± 0.8	Amp. Mod.
B1937−26	0.403	1904	...	...	...	...	...	...	...	...	Low emission
B1952+29	0.427	3512	...	...	...	...	0.039 ± 0.018	0.042	1.9	26 ± 12	Low emission
B2016+28	0.558	5358	...	...	...	...	...	...	...	...	No Nulls
B2021+51	0.529	5598	...	...	...	...	0.045 ± 0.030	0.070	5.5	22 ± 15	Low emission
B2043−04	1.547	1980	...	...	...	...	...	...	...	...	No Nulls
B2045−16	1.962	1199	9.2 ± 0.7	69	14.4	2.8	0.023 ± 0.013	0.031	25.5	43 ± 25	Periodic Nulls
B2053+21	0.815	2198	...	...	...	...	...	...	...	...	No Nulls
B2111+46	1.015	2000	8.7 ± 0.5	130	11.1	4.1	0.021 ± 0.005	0.011	70.4	48 ± 10	Periodic Nulls
B2217+47	0.538	2179	...	...	...	...	...	...	...	...	No Nulls
B2224+65	0.683	2049	...	...	...	...	...	...	...	...	Low emission
B2310+42	0.349	3583	5.1 ± 0.8	54	36.6	2.9	0.045 ± 0.015	0.034	11.4	22.3 ± 7.2	Periodic Nulls
B2319+60	2.256	2121	15.2 ± 1.1	100	15.0	6.2	0.017 ± 0.005	0.012	39.6	58 ± 17	Periodic Nulls
B2327−20	1.644	1854	10.7 ± 1.0	130	11.9	2.3	0.048 ± 0.023	0.054	13.3	20.8 ± 9.9	Periodic Nulls

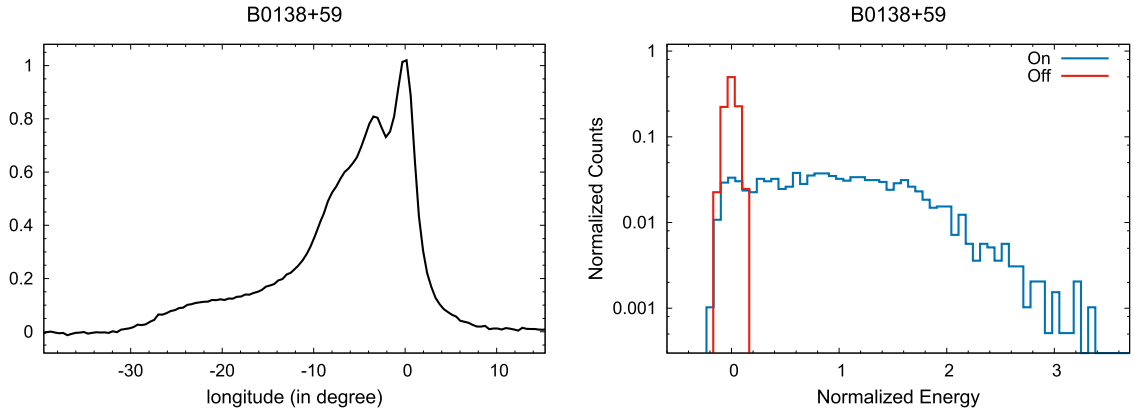

Figure 1. The figure shows the average profile (left panel) and pulse energy distribution (right panel) of the pulsar B0138+59.
(The complete figure set (62 images) is available.)

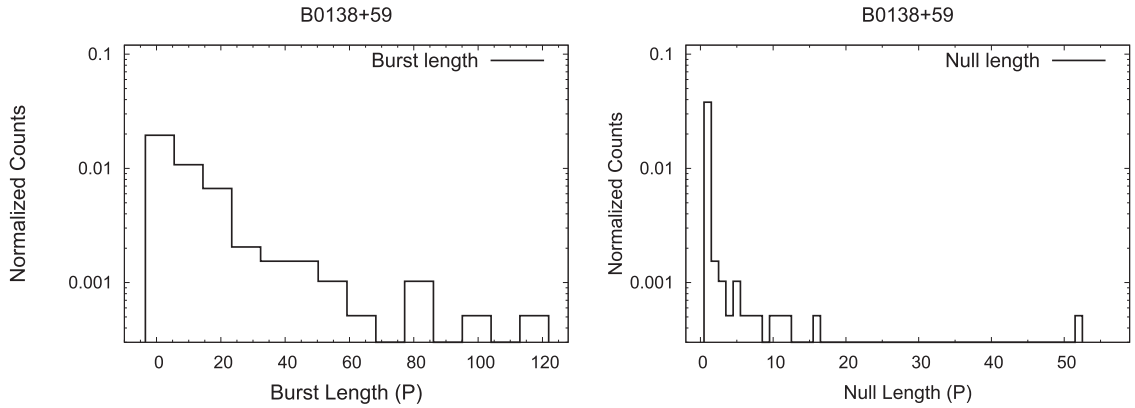

Figure 2. Burst length (left panel) and null length (right panel) distributions of the pulsar B0138+59.
(The complete figure set (17 images) is available.)

conducted an exhaustive literature survey. In Section 2 we describe details of observations from GMRT as well as analysis schemes used to determine nulling and periodic behavior. Section 3 carries out a collective study of all known pulsars showing periodic modulations, including those previously reported in the literature. A detailed discussion comparing the physical properties of different periodic behaviors in pulsars is presented in Section 4. Finally, Section 5 summarizes the primary results and conclusions of our studies.

2. Observations and Analysis

A large sample of pulsars was assembled by Basu et al. (2019a) to study drifting behavior in the population. This list included more than 30 pulsars observed with GMRT and another fifty from archival observations (Mitra & Rankin 2011). Many of these sources exhibited nulling and periodic modulations, whose properties we have explored in this work. We have carried out a detailed nulling and fluctuation spectral analysis of 62 pulsars, as shown in Table 1.

Pulsars were observed in "Phased-Array" mode at the 325 MHz frequency band. We analyzed sources without any previous studies of nulling or periodic modulation. Details for the observations and the instrumental setup are available in Basu et al. (2019a). Initially, recorded signals from each pulsar were converted into a well-calibrated, baseline-corrected, single pulse sequence (Basu et al. 2016; Mitra et al. 2016). Subsequently, a number of different analyses were carried out, which are briefly summarized below (Basu et al. 2017).

Nulling was studied by identifying suitable on-pulse and off-pulse windows in profile. Average energies in these windows were calculated for each pulse. The pulse energy distribution for the entire sequence was estimated to search for the presence of nulling. Figure 1 shows an example of on-pulse and off-pulse energy distributions for the nulling pulsar B0138+59. On-pulse energies show bimodal behavior, while null pulses are coincident with an off-pulse distribution. The nulling fraction (NF) was estimated by fitting Gaussian functions to the null and off-pulse distributions and finding suitable scaling relations between them (Ritchings 1976). The errors in NF were calculated from statistical errors of functional fits. In a few pulsars there were short-duration (a few periods), infrequent but clear nulls, which were too few to resemble fully formed Gaussian functions. In such cases the number of null pulses was individually counted to estimate NF. The errors in NF were estimated as $\delta\mathrm{NF} = \sqrt{n_p}/N_p$, where n_p corresponded to all null pulses and N_p is the total number of pulses.

In Table 1 we report 20 pulsars where nulling was present. In the list, 19 pulsars show clear separation between on-pulse and off-pulse distributions, indicating an absence of nulling. The last column in the Table identifies 17 pulsars without any nulling. In addition, two pulsars, B0450−18 and B1642−03, also had no detectable nulls. The detection sensitivities of the

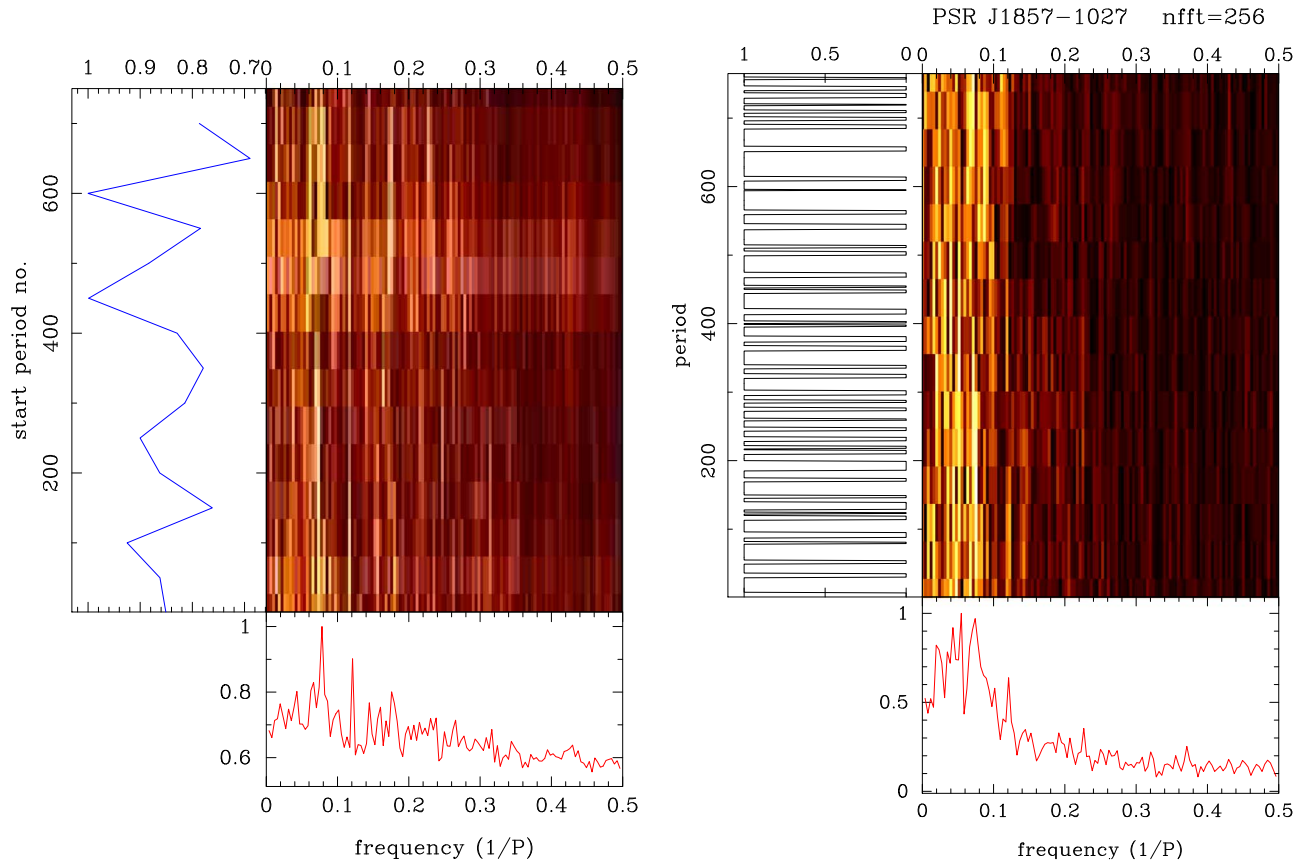

Figure 3. Time evolution of LRFS (left panel) and null-burst time series FFT (right panel) in the pulsar J1857−1027.
(The complete figure set (24 images) is available.)

single pulses in the remaining 23 pulsars were not sufficient to rule out the presence of nulling. Figure 2 shows an example of null length and burst length distributions for the pulsar B0138 +59. There were 17 pulsars where such distributions could be estimated. The table also lists the total number of transitions from null to burst sequence (N_T), as well as the average duration of nulls ($\langle$NL$\rangle$) and bursts ($\langle$BL$\rangle$) in these 17 pulsars.

We have also investigated the presence of periodic modulations in these pulsars. This involved determining time variations in LRFS as well as harmonic-resolved fluctuation spectra (HRFS, Deshpande & Rankin 2001), as described in Basu et al. (2016). In nulling pulsars with well-defined null and burst pulses, the presence of periodic nulling was also explored. Nulls were identified as "0" and bursts as "1" and the Fourier transforms of this binary series were determined (see Basu et al. 2017, for details). Figure 3 shows time-varying LRFS and nulling FFT in the pulsar J1857−1027 with periodic nulling.

Periodic modulations were detected in 24 pulsars, with 11 pulsars exhibiting periodic nulling and another 6 showing periodic amplitude modulations. The exact nature of periodic behavior in the remaining 7 pulsars was indeterminate due to the lower sensitivity of detections. Only 10 out of 17 pulsars with clearly separated null and burst pulses had periodic nulling. Additionally, the pulsar J1857−1027 showed the presence of clear nulls of 5–10P durations that were also periodic in nature (see Figure 3), but the emission was too weak for other nulling analysis. Table 1 reports peak modulation frequency (f_p), width of peak feature (FWHM), strength of the feature (S_M), defined as the relative height of feature from the baseline divided by FWHM, and periodicity (P_M). The error in the estimating peak frequency is given as $\delta f_p = \mathrm{FWHM}/2\sqrt{2\ln(2)}$ (Basu et al. 2016).

3. Pulsars with Periodic Modulations

We have investigated all known pulsars with periodic modulations that are different from subpulse drifting. There are around 70 pulsars exhibiting periodic behavior either in the form of periodic nulling, periodic amplitude modulations, or indeterminate cases. Individual pulsars belonging to each group are described below along with their basic physical properties.

3.1. Periodic Nulling

Table 2 presents 29 pulsars that exhibit periodic nulling. The table also describes the various physical characteristics of these pulsars, including their $\dot{E}$ values, nulling periodicity (P_N), profile classification, the presence of subpulse drifting and/or mode changing in pulse sequence, and references for the initial detection of periodic nulling in each pulsar. Periodic nulling was first detected in the pulsar B1133+16 by Herfindal & Rankin (2007) and subsequently its presence was reported in PSR J1819+1305 by Rankin & Wright (2008). Herfindal & Rankin (2009) identified nine additional pulsars with this behavior, which was further increased to a total of 19 pulsars by Basu et al. (2017, see Table 3 of this paper). Subsequently, periodic nulling was also detected in PSR B0823+26 (Basu & Mitra 2019), PSR B1819−22 (Basu & Mitra 2018b), and PSR

Table 2
Periodic Nulling

PSR	$\dot{E}$	P_N	Profile		Reference
	(2×10^{32} erg s^{-1})	(P)			
B0031−07	0.096	75 ± 14	S_d	Drift, Mode	(1)
B0138+59	0.042	44 ± 30	M	⋯	(2)
B0301+19	0.096	103 ± 34	D	Drift	(3)
B0525+21	0.151	46 ± 4	D	⋯	(3)
B0751+32	0.071	73 ± 10	D	⋯	(3)
B0823+26	2.260	14 ± 3	S_t	Mode	(4)
B0834+06	0.650	16 ± 4	D	Drift	(3)
B0932−52	0.305	35 ± 19	S_d	Drift	(2)
B1133+16	0.440	29 ± 2	D	⋯	(5)
B1237+25	0.072	26 ± 5	M	Drift, Mode	(2)
B1508+55	2.440	15 ± 7	T	⋯	(2)
J1649+2533	0.106	27 ± 2	⋯	⋯	(3)
B1706−16	4.470	130 ± 70	S_t	⋯	(1)
J1727−2739	0.101	206 ± 33	D	Drift	(1)
B1738−08	0.053	34 ± 8	$_c$Q?	Drift	(1)
J1819+1305	0.060	64 ± 8	$_c$Q	⋯	(6)
B1819−22	0.041	134 ± 33	D	Drift, Mode	(7)
J1857−1027	0.042	18 ± 10	T	⋯	(2)
B1905+39	0.057	47 ± 24	M	⋯	(2)
B1918+19	0.320	85 ± 14	$_c$T	Drift, Mode	(3)
B1944+17	0.056	600 ± 52	$_c$T	Drift, Mode	(1)
B2003−08	0.046	41 ± 4	M	Drift, Mode	(8)
B2034+19	0.045	57 ± 6	T	⋯	(3)
B2045−16	0.287	51 ± 20	T	Drift	(1)
B2111+46	0.135	48 ± 10	T	⋯	(2)
B2303+30	0.146	43 ± 8	S_d	Drift, Mode	(3)
B2310+42	0.520	32 ± 11	$_c$T	Drift	(1)
B2319+60	0.121	58 ± 17	$_c$Q	Drift, Mode	(2)
B2327−20	0.206	19 ± 1	T	⋯	(1)

References. (1) Basu et al. (2017), (2) This paper; (3) Herfindal & Rankin (2009), (4) Basu & Mitra (2019), (5) Herfindal & Rankin (2007), (6) Rankin & Wright (2008), (7) Basu & Mitra (2018b), (8) Basu et al. (2019b).

B2003−08 (Basu et al. 2019b). We have identified an additional 8 pulsars with periodic nulling in Table 1.

The physical characteristics of these pulsars indicate that periodic nulling coexists with subpulse drifting and mode changing. In this list there are 15 pulsars that show subpulse drifting and 9 pulsars also have multiple emission modes. In eight pulsars all three phenomena are seen in the same pulse sequence. Profile classifications show that periodic nulling is not restricted to any particular profile type but seen across all classes; $S_d = 3$; $S_t = 2$; D = 7; $_c$T = 3; $_c$Q = 3; T = 6; M = 4; not classified = 1.

3.2. Periodic Amplitude Modulation

We have identified 18 pulsars with periodic amplitude modulation; they are reported in Table 3. The table also describes the different physical characteristics of each pulsar, including $\dot{E}$, modulation periodicity (P_A), profile classification, and the presence of subpulse drifting and/or mode changing. These periodicities were measured in the works of Weltevrede et al. (2006, 2007), Basu et al. (2016) and this work, but they were not recognized as a separate phenomenon in previous studies.

Some of the interesting physical behaviors of periodic amplitude modulation are summarized below. The pulsar B0823+26 has periodic amplitude modulation during its B mode, while the Q mode shows periodic nulling (Basu & Mitra 2019). The two modes in PSR B1822−09 have periodic amplitude modulation with different periodicities (Latham et al. 2012; Hermsen et al. 2017; Yan et al. 2019). PSR B1737+13 shows drifting in its conal components (Force & Rankin 2010).

Table 3
Periodic Amplitude Modulation

PSR	$\dot{E}$	P_A	Profile	
	(2×10^{32} erg s^{-1})	(P)		
B0450−18	6.850	16 ± 6	T	⋯
B0450+55	11.850	9 ± 1	T	⋯
B0823+26	2.260	6 ± 1	S_t	Mode
B1055−52	150.500	21 ± 2	⋯	⋯
B1541+09	0.204	15 ± 5	T	⋯
B1600−49	5.750	50 ± 26	T	⋯
B1604−00	0.805	34 ± 13	T	⋯
B1642−03	6.050	13 ± 4	S_t	⋯
B1718−32	1.175	23 ± 9	$T_{1/2}$	⋯
B1732−07	3.250	20 ± 8	T	⋯
B1737+13	0.555	∼90	M	Drift
B1737−39	2.835	10 ± 4	T	⋯
B1745−12	3.910	7 ± 1	T	⋯
B1822−09	22.800	46 ± 1	$T_{1/2}$	Mode
B1845−01	3.615	20 ± 8	$_c$T	⋯
B1917+00	0.735	11 ± 0.4	T	⋯
B1929+10	19.650	12 ± 1	S_t	⋯
B1946+35	3.775	50 ± 10	T	⋯

Table 4
Periodic Modulation (Unresolved)

PSR	$\dot{E}$	P_M	Profile	
	(2×10^{32} erg s^{-1})	(P)		
B0621−04	0.146	73 ± 2	M	Drift
B0756−15	1.005	23 ± 10	$T_{1/2}$	···
B1114−41	1.87	36 ± 14	S_t	···
B1510−48	1.94	37 ± 4	···	Drift
J1603−2531	13.85	69 ± 28	S_t	···
B1601−52	0.178	21 ± 7	D	···
J1650−1654	0.118	64 ± 45	D	Drift
B1700−18	0.655	43 ± 15	···	Drift
B1702−19	30.55	11 ± 0.4	$T_{1/2}$	
B1730−37	77.0	71 ± 20	···	
B1753+52	0.023	11 ± 5	$_cQ$	···
B1758−03	0.835	81 ± 42	$T_{1/2}$	···
B1839+56	0.066	40 ± 20	···	···
B1839+09	3.88	37 ± 3	S_t	···
B1859+01	19.45	14 ± 1	T	···
B1907+10	22.85	13 ± 2	S_t	···
B1911−04	1.425	15 ± 5	S_t	···
B1952+29	0.004	26 ± 12	M/T?	···
B1953+50	1.94	25 ± 7	S_t	···
B2011+38	143.0	30 ± 15	···	···
B2021+51	4.08	22 ± 15	D	···
B2106+44	0.239	19 ± 7	···	···
B2255+58	22.75	10 ± 1	S_t	···
J2346−0609	0.163	100 ± 30	D	···

Periodic amplitude modulation is seen primarily in profiles with central LOS traversals, where usually prominent core emission is present. The numbers of pulsars belonging to different profile types are estimated as: $S_t = 3$; $_cT = 1$; $T_{1/2} = 2$; T = 10; M = 1; not classified = 1.

3.3. Unresolved Modulation

Twenty-four pulsars show clear periodicities in their single-pulse sequence, but their detection sensitivities are insufficient to determine the exact nature of modulation. Table 4 shows the basic physical properties of these pulsars, including $\dot{E}$, modulation periodicity (P_M), profile classification, and the presence of subpulse drifting. Mode changing is not seen in any of these sources. Four pulsars in this group, PSR B0621−04, B1510−48, J1650−1654, and B1700−18 also have subpulse drifting. Their profiles show a wide variety: $S_t = 7$; D = 4; $_cQ = 1$; $T_{1/2} = 3$; T = 1 or 2; M = 1 or 2; not classified = 6.

There are an additional 20-30 pulsars where periodic behavior was also reported in earlier works (Weltevrede et al. 2006, 2007). In eight of them, PSR B0329+54, B0402+61, B0919+06, B0950+08, B1112+50, B1612+07, B1937−26, and B2217+47 we did not find any clear modulation features in the fluctuation spectra. In the remaining cases more sensitive observations are required to validate the presence of periodic behavior.

4. Periodic Modulation: Distinct Physical Phenomenon

Major differences between periodic modulations and subpulse drifting are summarized in Table 5. We have estimated the dependence of modulation periodicity (P_M) with $\dot{E}$, which is shown in Figure 4. The figure represents the P_M of three groups,

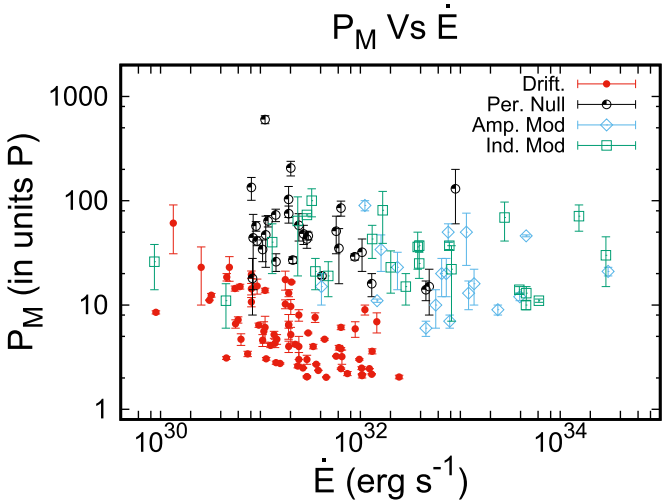

Figure 4. Modulation periodicities (P_M) of pulsars, along with their spin-down energy loss ($\dot{E}$). Periodic nulling (black open circles), periodic amplitude modulation (blue rhombus), and indeterminate periodic modulations (green square) are shown in the figure, along with subpulse drifting (red filled circles) for comparison. The three periodic modulations overlap along the $\dot{E}$ axis, underlining their common physical origin. Subpulse drifting, on the other hand, demonstrates different physical behavior. It is seen for a limited region along the $\dot{E}$ axis ($\leqslant 2 \times 10^{32}$ erg s^{-1}) and is weakly anti-correlated with $\dot{E}$.

periodic nulling (black open circles), periodic amplitude modulation (blue rhombus), and indeterminate periodic modulation (green square), defined in the previous section, along the $\dot{E}$ axis. Drifting periodicities (red filled circles) are also shown for comparisons. The figure highlights two primary features, a clear distinction between subpulse drifting and other periodic modulations, and overlapping behavior between the three groups of periodic modulations.

Physical differences between subpulse drifting and other periodic modulations are also seen in their distributions of periodicity and $\dot{E}$. Periodic modulations (Figure 5, left panel) have typical periodicities between 10 and 200P, the distribution peaking around 50P, and there are very few exceptions, around five cases, outside this range. On the other hand, subpulse drifting has a periodicity below 20P in most cases, with the distribution peaking around 5P. Longer periodic drifting is usually seen for low $\dot{E}$ pulsars. One of the primary limitations of measuring periodic phenomena in pulsars, particularly short periodicities, is the aliasing effect around 2P. This is reflected in the sharp cutoff at the lower part of the drifting periodicity distribution, possibly skewing it toward longer periodicities. The $\dot{E}$ distributions (Figure 5, right panel) of the two populations also show very different behaviors. Subpulse drifting peaks around 3×10^{31} erg s^{-1}, with an upper cutoff around 2×10^{32} erg s^{-1}. In contrast, periodic modulations are seen over a much wider $\dot{E}$ range, with a plateau between 10^{31} and 10^{34} erg s^{-1}.

Both periodic nulling and periodic amplitude modulation share a number of identical features. This includes a lack of any dependence of their periodicities on $\dot{E}$, the presence across the entire profile including core emission, and longitude-stationary behavior in all components. These suggest that their underlying physical processes are also likely similar. We propose that they represent a class of newly emergent emission behavior in pulsars with distinct physical mechanisms compared to subpulse drifting.

Table 5
Comparing Periodic Behavior in Pulsar Radio Emission

	Subpulse Drifting	Periodic Modulations
Profile component	(i) Only seen in conal components.	(i) Simultaneously seen in central core and cones.
	(ii) Different phase variations for different components.	(ii) longitude-stationary, similar across all components.
Spin-down energy	(i) Seen in pulsars with $\dot{E} < 5 \times 10^{32}$ erg s^{-1}.	(i) Seen in pulsars with wide $\dot{E}$ distribution.
	(ii) P_3 weakly anti-correlated with $\dot{E}$.	(ii) $P_M \sim$ 10–200P, no dependence of P_M on $\dot{E}$.
Origin	(i) Localized in Inner Acceleration Region.	(i) Seen in both poles of pulsars with interpulse emission.
	(ii) Associated with sparking process of plasma generation.	(ii) Large-scale variations affecting pulsar magnetosphere.

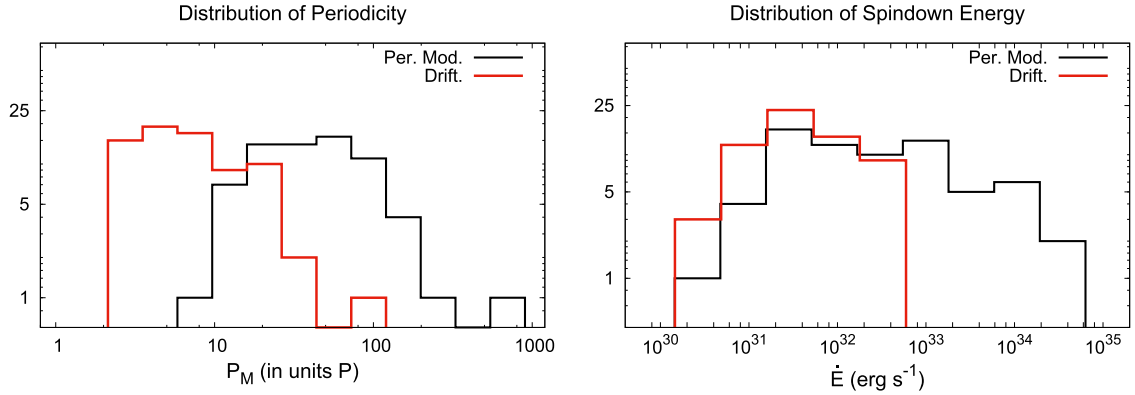

Figure 5. Distributions of modulation periodicity (left panel) and spin-down energy loss (right panel) for subpulse drifting and other periodic modulations. A clear distinction is seen between the two populations in both plots. Subpulse drifting is seen in pulsars with $\dot{E} < 2 \times 10^{32}$ erg s^{-1}, while periodic modulations are seen along a wider $\dot{E}$ range. Subpulse drifting usually has lower periodicities, with only a small fraction exceeding 20P. On the other hand, modulation periodicities are usually longer, with typical values between 10 and 200P.

We have also compared the physical properties of pulsars with periodic nulling and the general nulling population. A detailed literature survey of nulling is reported in Table 6, which lists pulsar names, $\dot{E}$, NF, reference for NF, and profile type. Only traditional nulling pulsars are considered for comparisons and more extreme examples like intermittent pulsars are not included. We have also excluded sources where only the upper limits of NF are reported due to lower-sensitivity detections. This left 83 pulsars where nulling is unambiguously observed.

No clear trends emerge for nulling, either in NF or their profile types. The $\dot{E}$ distribution of all nulling pulsars is shown in Figure 6, along with the distribution for periodic nulling. There is no sharp cutoff seen in the $\dot{E}$ distributions, unlike subpulse drifting. However, nulling becomes less prevalent in high $\dot{E}$ pulsars, with no nulling seen above 10^{34} erg s^{-1}. The figure also shows that the distribution of periodic nulling pulsars cannot be distinguished from the non-periodic case.

It is likely that periodic nulling is more prevalent than the 29 cases reported here, and more sensitive single pulse studies in the future will increase this number. For example, in three pulsars, B1114−41, B1758−03, and J2346−0609, the presence of periodic behavior is seen in fluctuation spectra, but the detection sensitivities of single pulses were not sufficient to ascertain periodic nulls. However, there are also several examples where sensitive single-pulse studies could not detect the presence of any periodicity associated with nulling. We did not detect periodicity in 7 out of a possible 17 pulsars studied here. Basu et al. (2017, see Table 2) also reported eight pulsars without any periodic nulling, despite sensitive single-pulse detections. Currently, periodic nulling is seen in around 35% of nulling pulsars.

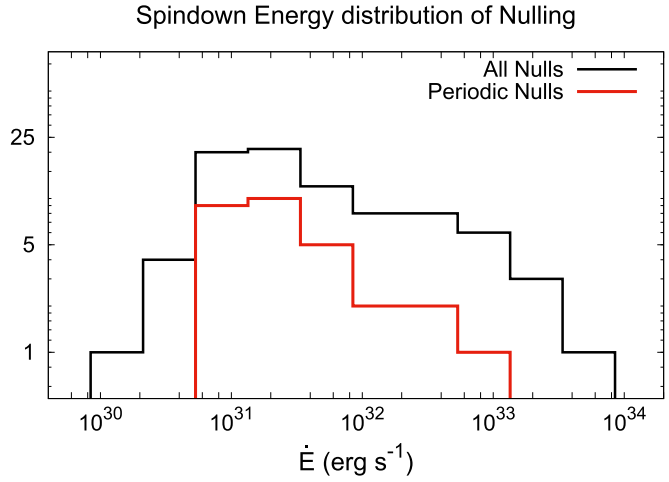

Figure 6. $\dot{E}$ distribution of pulsars showing the presence of nulling in their single pulse sequences. The black histograms show the distribution for the entire nulling population, while the red plot corresponds to the subgroup showing periodic nulling.

5. Summary and Conclusion

In this paper we have carried out a detailed study of periodic amplitude modulation and periodic nulling seen in single pulse sequences of many normal period ($P > 0.1$ s) pulsars. A complete list of all possible sources was compiled from the literature as well as newer observations using GMRT. We have carried out detailed nulling and periodic modulation analysis in 62 pulsars. Our studies found nulling in 20 pulsars and periodic modulations in 24 cases. We detected periodic nulling in 10 pulsars, 8 of which were new detections, expanding this population to 29 pulsars. We have identified 18 pulsars that

Table 6
Nulling in Pulsars

PSR	$\dot{E}$ (2×10^{32} erg s^{-1})	NF (%)	Profile	Reference	PSR	$\dot{E}$ (2×10^{32} erg s^{-1})	NF (%)	Profile	Reference
B0031−07	0.096	37.7	S_d	(1)	B1738−08	0.053	15.8 ± 1.4	$_c$Q	(5)
B0045+33	0.258	21	⋯	(2)	B1742−30	42.45	32.5 ± 1.2	M	(5)
B0138+59	0.042	7.6 ± 1.0	M	(3)	B1747−46	0.625	2.4 ± 0.5	S_t	(5)
B0301+19	0.096	7.4 ± 0.7	D	(4)	J1752+2359	1.855	75	⋯	(15)
B0320+39	0.005	0.7 ± 0.2	$_c$T	(3)	B1749−28	0.009	1.0 ± 0.4	T	(5)
B0525+21	0.151	28 ± 2	D	(4)	B1758−03	0.835	26.9 ± 1.6	T	(5)
B0628−28	0.73	13.6 ± 1.9	S_d	(5)	J1808−0813	0.364	10.8 ± 1.1	S_d	(5)
B0751+32	0.071	38 ± 6	D	(4)	B1809−173	2.15	5.8 ± 4	S_t	(10)
B0809+74	0.015	1.2 ± 0.4	S_d	(3)	B1813−36	6.95	16.7 ± 0.7	T	(5)
B0818−13	0.219	0.9 ± 0.1	S_d	(3)	J1819+1305	0.060	41 ± 6	$_c$Q	(4)
B0820+02	0.032	0.5 ± 0.2	S_d	(3)	J1820−0509	4.795	67 ± 3	⋯	(10)
B0823+26	2.26	3.85 ± 0.05	S_t	(6)	B1819−22	0.041	5.5 ± 0.2	D	(16)
B0834+06	0.65	4.4 ± 0.4	D	(5)	J1831−1223	0.046	4 ± 1	⋯	(10)
B0906−17	2.04	12.4 ± 1.1	T	(3)	J1840−0840	0.031	50 ± 6	D	(17)
J0930−2301	0.113	>30	⋯	(7)	B1845−19	0.058	27.2 ± 1.7	T	(3)
B0932−52	0.305	1.9 ± 0.1	S_d	(3)	B1848+12	1.30	51 ± 2	S_t	(4)
B0940−55	15.4	<12.5	S_t	(8)	J1857−1027	0.042	>30	T	(3)
B0940+16	0.014	8 ± 3	T	(9)	B1857−26	0.176	4.3 ± 0.5	M	(3)
B0942−13	0.048	14.4 ± 0.9	$T_{i/2}$	(5)	J1901−0906	0.057	3.8 ± 0.7	D	(5)
J1049−5833	0.082	47 ± 3	⋯	(10)	B1905+39	0.057	10.0 ± 0.5	M	(3)
B1112+50	0.109	34.8 ± 1.4	$T_{i/2}$	(3)	B1907+03	0.070	4 ± 0.2	T/M	(9)
B1114−41	1.87	3.3 ± 0.5	S_t	(5)	J1920+1040	0.118	50 ± 4	⋯	(10)
B1133+16	0.440	13 ± 2	D	(5)	B1918+19	0.320	2.0 ± 0.3	$_c$T	(5)
B1237+25	0.072	2.5 ± 0.1	M	(5)	J1926−1314	0.063	74 ± 2	⋯	(18)
B1322−66	6.55	9.1 ± 3	⋯	(10)	B1942+17	0.018	60	D	(19)
B1325−49	0.037	4.2 ± 0.3	M	(5)	B1942−00	0.093	21 ± 1	D	(9)
B1358−63	5.50	1.6 ± 1	⋯	(10)	B1944+17	0.056	32.0 ± 1.6	$_c$T	(5)
J1502−5653	2.35	93 ± 4	⋯	(10)	B2003−08	0.046	28.6 ± 3.4	M	(20)
B1508+55	2.44	5.2 ± 0.4	T	(3)	B2034+19	0.045	44 ± 4	T	(4)
J1525−5417	3.085	16 ± 5	⋯	(10)	B2045−16	0.287	8.8 ± 0.6	T	(5)
B1524−39	0.267	5.1 ± 1.3	D	(5)	B2110+27	0.298	30	S_d	(2)
B1530+27	0.108	6 ± 2	S_d	(9)	B2111+46	0.135	8.7 ± 0.5	T	(3)
B1604−00	0.805	0.15 ± 0.07	T	(3)	B2122+13	0.454	22	D	(2)
J1649+2533	0.106	25 ± 5	⋯	(4)	B2154+40	0.191	7.5 ± 2.5	$_c$T	(21)
B1658−37	0.149	14 ± 2	⋯	(10)	J2253+1516	0.026	49	D	(2)
J1702−4428	0.068	26 ± 3	⋯	(10)	B2303+30	0.146	5.3 ± 0.5	S_d	(5)
B1700−32	0.073	0.9 ± 0.2	T	(5)	B2310+42	0.52	4.5 ± 0.6	$_c$T	(3)
B1706−16	4.47	31 ± 2	S_t	(11)	B2315+21	0.069	3 ± 0.5	$_c$T	(9)
B1713−40	1.04	80 ± 15	S_t	(12)	B2319+60	1.21	15.2 ± 1.1	$_c$Q	(3)
J1725−4043	0.175	<70	⋯	(13)	B2327−20	0.206	11.2 ± 1.0	T	(3)
J1727−2739	0.101	68.2 ± 1.1	D	(14)	J2346−0609	0.163	35.6 ± 2.2	D	(5)
J1738−2330	0.218	>69	⋯	(13)					

References. (1) Huguenin et al. (1970), (2) Redman & Rankin (2009), (3) This paper; (4) Herfindal & Rankin (2009), (5) Basu et al. (2017), (6) Basu & Mitra (2019), (7) Kawash et al. (2018), (8) Biggs (1992), (9) Weisberg et al. (1986), (10) Wang et al. (2007), (11) Naidu et al. (2018), (12) Kerr et al. (2014), (13) Gajjar et al. (2012), (14) Wen et al. (2016), (15) Lewandowski et al. (2004), (16) Basu & Mitra (2018b), (17) Gajjar et al. (2017), (18) Rosen et al. (2013), (19) Lorimer et al. (2002), (20) Basu et al. (2019b), (21) Ritchings (1976).

exhibit periodic amplitude modulation, not associated with nulling, which is the first such categorization of this behavior. Additionally, we have also identified 24 pulsars with periodic modulation, where detection sensitivities were insufficient to distinguish between the two phenomena.

Most periodic modulations have been considered a form of subpulse drifting in a majority of past studies. We have compared periodic behavior associated with subpulse drifting and other periodic modulations and found them to exhibit different physical properties. The different periodic modulations exhibit similar characteristics, like overlapping periodicities along $\dot{E}$ and longitude-stationary behavior across all profile components, which suggest similar physical mechanisms. We have also found periodic nulling to be a significant subset of the nulling phenomenon in general, with no clear distinctions in physical properties.

We thank the referee for the comments which helped to improve the paper. D.M. acknowledges funding from the Indo-French Centre for the Promotion of Advanced Research (CEFIPRA): grant IFC/F5904-B/2018. We thank the staff of the GMRT, who made these observations possible. The GMRT is run by the National Centre for Radio Astrophysics of the Tata Institute of Fundamental Research.

ORCID iDs

Rahul Basu https://orcid.org/0000-0003-1824-4487
Dipanjan Mitra https://orcid.org/0000-0002-9142-9835
Giorgi I. Melikidze https://orcid.org/0000-0003-1879-1659

References

Backer, D. C. 1970a, Natur, 228, 692
Backer, D. C. 1970b, Natur, 228, 42
Backer, D. C. 1970c, Natur, 228, 1297
Backer, D. C. 1973, ApJ, 182, 245
Basu, R., & Mitra, D. 2018a, MNRAS, 475, 5098
Basu, R., & Mitra, D. 2018b, MNRAS, 476, 1345
Basu, R., & Mitra, D. 2019, MNRAS, 487, 4536
Basu, R., Mitra, D., Melikidze, G. I., et al. 2016, ApJ, 833, 29
Basu, R., Mitra, D., & Melikidze, G. I. 2017, ApJ, 846, 109
Basu, R., Mitra, D., Melikidze, G. I., & Skrzypczak, A. 2019a, MNRAS, 482, 3757
Basu, R., Paul, A., & Mitra, D. 2019b, MNRAS, 486, 5216
Becker, W. 2009, ASSL, 357, 91
Biggs, J. D. 1992, ApJ, 394, 574
Deshpande, A. A., & Rankin, J. M. 2001, MNRAS, 322, 438
Drake, F. D., & Craft, H. D. 1968, Natur, 220, 231
Force, M. M., & Rankin, J. M. 2010, MNRAS, 406, 237
Gajjar, V., Joshi, B. C., & Kramer, M. 2012, MNRAS, 424, 1197
Gajjar, V., Yuan, J. P., Yuen, R., et al. 2017, ApJ, 850, 173
Gil, J., Melikidze, G. I., & Geppert, U. 2003, A&A, 407, 315
Gil, J., & Sendyk, M. 2000, ApJ, 541, 351
Goldreich, P., & Julian, W. H. 1969, ApJ, 157, 869
Herfindal, J. L., & Rankin, J. M. 2007, MNRAS, 380, 430
Herfindal, J. L., & Rankin, J. M. 2009, MNRAS, 393, 1391
Hermsen, W., Kuiper, L., Hessels, J. W. T., et al. 2017, MNRAS, 466, 1688
Huguenin, G. R., Taylor, J. H., & Troland, T. H. 1970, ApJ, 162, 727
Kawash, A. M., et al. 2018, ApJ, 857, 131
Kerr, M., Hobbs, G., Shannon, R. M., et al. 2014, MNRAS, 445, 320
Latham, C., Mitra, D., & Rankin, J. 2012, MNRAS, 427, 180
Lewandowski, W., Wolszczan, A., Feiler, G., Konacki, M., & Soltysinski, T. 2004, ApJ, 600, 905
Lorimer, D. R., Camilo, F., & Xilouris, K. M. 2002, AJ, 123, 1750
Mitra, D., Arjunwadkar, M., & Rankin, J. 2015, ApJ, 806, 236
Mitra, D., Basu, R., Maciesiak, K., et al. 2016, ApJ, 833, 28
Mitra, D., & Rankin, J. 2017, MNRAS, 468, 4601
Mitra, D., & Rankin, J. M. 2011, ApJ, 727, 92
Naidu, A., Joshi, B. C., Manoharan, P. K., & Krishnakumar, M. A. 2018, MNRAS, 475, 2375
Rankin, J. M. 1986, ApJ, 301, 901
Rankin, J. M. 1990, ApJ, 352, 247
Rankin, J. M. 1993, ApJ, 405, 285
Rankin, J. M., Rodriguez, C., & Wright, G. A. E. 2006, MNRAS, 370, 673
Rankin, J. M., & Wright, G. A. E. 2008, MNRAS, 385, 1923
Redman, S. L., & Rankin, J. M. 2009, MNRAS, 395, 1529
Ritchings, R. T. 1976, MNRAS, 176, 249
Ritchings, R.T., & Lyne, A.G. 1975, Natur, 257, 293
Rosen, R., et al. 2013, ApJ, 768, 85
Ruderman, M. A., & Sutherland, P. G. 1975, ApJ, 196, 51
Szary, A. 2013, PhD thesis, Univ. Zielona Góra, arXiv:1304.4203
Szary, A., Melikidze, G. I., & Gil, J. 2015, MNRAS, 447, 2295
Wahl, H. M., Orfeo, D. J., Rankin, J. M., & Weisberg, J. M. 2016, MNRAS, 461, 3740
Wang, N., Manchester, R. N., & Johnston, S. 2007, MNRAS, 377, 1383
Weisberg, J. M., Armstrong, B. K., Backus, P. R., et al. 1986, AJ, 92, 621
Weltevrede, P., Edwards, R. T., & Stappers, B. W. 2006, A&A, 445, 243
Weltevrede, P., Edwards, R. T., & Stappers, B. W. 2007, A&A, 469, 607
Wen, Z. G., Wang, N., Yuan, J. P., et al. 2016, A&A, 592, 127
Yan, W. M., Manchester, R. N., Wang, N., et al. 2019, MNRAS, 485, 3241